# Energy and Exergy Analysis of an Ejector-Absorption Refrigeration Cycle with Using $NH_3$-$H_2O$ as the Working Fluids

**A. Habibzadeh[1, *], S. Jafarmadar[1], M. M. Rashidi[2], S. S. Rezaei[3], A. Aghagoli[3]**

*[1] Department of Mechanical Engineering, Engineering Faculty, Urmia University, Urmia, Iran.*
*[2]Department of Civil Engineering, University of Birmingham, Edgbaston, Birmingham, England.*
*[3] Department of Mechanical Engineering, Engineering Faculty, Bu Ali Sina University, Hamedan, Iran.*
*Received: 12 June 2017 - Accepted: 10 August 2017*

**Abstract**

In this paper, the thermodynamic simulation and the first and second laws analysis of an ammonia-water ejector-absorption refrigeration cycle is presented. A computer program has been applied in order to investigate the effects of parameters such as condenser, absorber, generator, and evaporator on the performance coefficient and exergy efficiency of this cycle. The results showed that in general when the temperature of different parts increases, performance coefficient and the exergy efficiency of the cycle decreases except for evaporator and generator that causes an increase in COP. The Entrainment ratio of the ejector, COP and exergy efficiency of the cycle decreases when the condenser temperature rises. Evaporator temperature increase leads to the increase of all studied parameters except exergy efficiency. Moreover, absorber and ejector have the highest exergy losses in the studied conditions. When generator temperature rises, total exergy loss and the entrainment ratio increase but leads to the reduction of the exergy efficiency.

*Keywords:* Absorption Refrigeration, Ejector, Exergy Efficiency, COP.

| **Nomenclature** | | | **12** | $\dot{W}$ | power rate, kW | **22** | $CON$ | condenser |
|---|---|---|---|---|---|---|---|---|
| **1** | $A$ | area, $m^2$ | **13** | $x$ | mass fraction of $NH_3$–$H_2O$ in solution | **23** | $EJE$ | ejector |
| **2** | $COP$ | the coefficient of performance | **Greek symbols** | | | **24** | $EVA$ | evaporator |
| **3** | $\dot{E}$ | exergy destruction rate, kW | **14** | $\Delta$ | difference | **25** | $exe$ | exergy |
| **4** | $h$ | specific enthalpy, $kJ\ kg^{-1}$ | **15** | $\eta$ | efficiency | **26** | $EXV$ | expansion valve |
| **5** | $\dot{m}$ | mass flow rate, $kg\ s^{-1}$ | **16** | $\varepsilon$ | the effectiveness of the heat exchanger | **27** | $GEN$ | generator |
| **6** | $P$ | pressure , $bar$ | **17** | $\mu$ | entrainment ratio of the ejector | **28** | $HE$ | heat exchanger |
| **7** | $\dot{Q}$ | heat transfer rate, kW | **18** | $\nu$ | specific volume, $m^3kg^{-1}$ | **29** | $mix$ | mixing |
| **8** | $Qu$ | quality | **Subscripts** | | | **30** | $p$ | pump |
| **9** | $s$ | specific entropy, $kJkg^{-1}K^{-1}$ | **19** | $0$ | reference environment | **31** | $pr$ | primary flow |
| **10** | $T$ | temperature, $^{\circ}C$ | **20** | $1,2,...$ | cycle locations | **32** | $sc$ | secondary flow |
| **11** | $V$ | velocity, $ms^{-1}$ | **21** | $ABS$ | absorber | **33** | $Total$ | total |

**Corresponding author*
*Email address: a.habibzadeh@urmia.ac.ir*

## 1. Introduction

In recent years, the use of absorption refrigeration cycles has increased remarkably, in spite of its lower performance compared to other refrigeration cycles. An absorption cycle does not use any mechanical energy for refrigeration or heat pumping, and only heat energy is applied. Therefore, it can be driven by low-grade heat energy.

Interest in absorption refrigeration technology has been growing because these systems do not deplete the ozone layer [1, 2]. Moreover, the ejectors are used in different engineering applications. As they have advantages over conventional compression systems, they can be used instead of compressors. Apart from a small liquid pump, the cycle has no moving parts and hence, there is no need for lubrication. Kairouani et al. [3] studied the performance of compression-absorption refrigeration (cascade) cycles. $NH_3$-$H_2O$ fluid pair was used at the absorption section of the refrigeration cycle, while three different working fluids (R717, R22, and R134a) were used at the vapor compression section. They showed that the COP can be improved by 37–54%, compared with the conventional cycle, under the same operating conditions.

Ammonia-water and water-lithium bromide are the common working fluids that are used in absorption refrigeration cycles. These fluids are used to achieve low temperatures (below $0^{o}C$) by using low-potential heat sources (70-120$^{o}C$) [4]. Lee and Sherif [5] analyzed absorption systems for cooling and heating applications. Second low analysis of an absorption water- lithium bromide refrigeration cycle was given by Talbi and Agnew [6]. Hong et al. [7] studied the performance of ejector-absorption combined refrigeration cycle. They showed that the COP of the cycle is 30% higher than that of the conventional single-effect absorption refrigeration cycle at the same working conditions. Vereda et al. [8] studied numerical model of an ejector-absorption (single-effect) refrigeration cycle with ammonia–lithium nitrate solution as working fluid. The results showed that the use of an ejector allows, among others, to decrease the activation temperature approximately 9 $^{\circ}C$ in respect to the conventional single-effect absorption cycle and increasing the COP for moderate temperatures. Alexis and Rogdakis [9] described the performance of an ammonia-water combined ejector-absorption cycle using two simple models. The first model COP varied from 1.099 to 1.355 and the second model COP varied from 0.247 to 0.382. Sözen et al. [10] studied an experimental analysis on performance improvement of a diffusion absorption refrigeration system (DARS). Experimental results showed that the DARS-1WE cycle demonstrates a higher performance compared to DARS-1 and DARS-2 cycles. Other studies about refrigeration cycles have been done by some researchers [11-24].

The aim of the present article is to investigate the temperature change in different parts of the ejector-absorption cycle and find its effect on different parameters such as COP, exergy efficiency, entrainment ratio and exergy loss.

## 2. The analysis of the Cycle

Fig. 1. shows the schematic of ejector-absorption cycle using $NH_3$-$H_2O$ as working fluid.

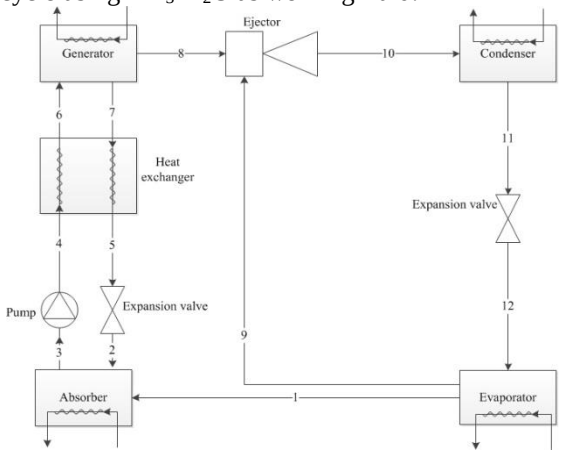


**Fig. 1. Schematic diagram of the ammonia- water absorption cycle.**

This cycle consists of five important parts: generator, evaporator, condenser, absorber and ejector and operates with only two pressure levels including high pressure in the generator and condenser and low pressure in the absorber and evaporator. At absorber pressure, the strong solution is pumped from the absorber toward the generator, which is at higher pressure, after passing through the solution heat exchanger and then is heated by the hot weak solution. At the generator, external heat is supplied in order to release the refrigerant vapor from the strong solution. After that, the refrigerant vapor in the generator enters the primary nozzle of the ejector. After passing the diffuser section of the ejector, and mixing with the flow from the evaporator, the refrigerant enters the condenser and is condensed to be saturated liquid, rejecting heat to the ambient. After an isenthalpic process, the low pressure and temperature flow that enters the evaporator is vaporized by absorbing heat from the cooled media and produces the necessary cooling effect. The vapor out from the evaporator exit is divided into two streams. One stream enters the secondary nozzle of the ejector and is mixed with the primary flow in the mixing chamber and the other stream enters the absorber at the evaporator pressure and rejects heat to the ambient.

### 2.1. Thermodynamic model

The thermodynamic analysis of the cycle was performed by using the following assumptions:

1. The system is in steady state.
2. All the pressure losses in the system are neglected.
3. Refrigerants are in saturated states at condenser, evaporator and absorber exit, $x_1 = x_8 = x_9 = x_{10} = x_{11} = 1$
4. The velocity at inlet and outlet of the ejector is neglected.
5. The inner wall of the ejector is adiabatic.

The calculation of the thermal capacities can be done by writing the mass and energy balance of each component in the cycle as the following equations.

### 2.2. First and second law analysis

Exergy is the most fundamental term in thermodynamics. Exergy is the maximum theoretical work that could be done by a system. The concept of exergy is discussed by Szargut et al. [25] and Bejan [26].

#### 2.2.1. Ejector

The ejector is the key part of this cycle that works based on the changes between the velocity and pressure.

The isentropic processes for the inlet of ejector can be expressed as:

$$h_9 = h_{9sc} + 0.5V_{9sc}^2 \quad (1)$$

$$h_8 = h_{8pr} + 0.5V_{8pr}^2 \quad (2)$$

The mass, momentum and energy conservations for the mixing chamber of ejector are calculated by the following equations:

$$\dot{m}_{mix} = \dot{m}_8 + \dot{m}_9 \quad (3)$$

$$P_{9sc}A_{mix} + \dot{m}_9 V_{9sc} + \dot{m}_8 V_{8pr} = P_{mix}A_{mix} + \dot{m}_{mix}V_{mix} \quad (4)$$

$$\dot{m}_9(h_{9sc} + 0.5V_{9sc}^2) + \dot{m}_{8pr}(h_{8pr} + 0.5V_{8pr}^2) = \dot{m}_{mix}(h_{mix} + 0.5V_{mix}^2) \quad (5)$$

The isentropic process for the inlet of ejector can be expressed as:

$$h_{10} = h_{mix} + 0.5V_{mix}^2 \quad (6)$$

The entrainment ratio of ejector can be expressed as:

$$\mu = \frac{\dot{m}_{sc}}{\dot{m}_{pr}} \quad (7)$$

The exergy loss of the ejector is calculated by:

$$\Delta\dot{E}_{EJE} = \dot{m}_9(h_9 - T_0 s_9) + \dot{m}_8(h_8 - T_0 s_8) - \dot{m}_{10}(h_{10} - T_0 s_{10}) \quad (8)$$

As it is known, in the compression refrigeration cycles, specifying two parameters is sufficient to find other thermodynamic properties of working fluids such as R134a, R12 and etc, but in the absorption refrigeration cycles that their working fluid is the mixture of $NH_3$-$H_2O$, determining three parameters is necessary to calculate other thermodynamic properties.

The thermodynamic properties of each component are given by the following equations.

#### 2.2.2. Generator

$$h_8 = f(T_{GEN}, Qu_{GEN}, x_{GEN}) \quad (9)$$

$$s_8 = f(T_{GEN}, Qu_{GEN}, x_{GEN}) \quad (10)$$

$$h_7 = f(T_{GEN}, Qu_{GEN}, P_{GEN}) \quad (11)$$

$$s_8 = f(T_{GEN}, Qu_{GEN}, P_{GEN}) \quad (12)$$

#### 2.2.3. Evaporator

$$h_{EVA} = f(T_{EVA}, Qu_{EVA}, x_{EVA}) \quad (13)$$

$$s_{EVA} = f(T_{EVA}, Qu_{EVA}, x_{EVA}) \quad (14)$$

#### 2.2.4. Condenser

$$h_{CON} = f(T_{CON}, Qu_{CON}, x_{CON}) \quad (15)$$

$$s_{CON} = f(T_{CON}, Qu_{CON}, x_{CON}) \quad (16)$$

#### 2.2.5. Absorber

$$h_{ABS} = f(T_{ABS}, P_{ABS}, Qu_{ABS}) \quad (17)$$

$$s_{ABS} = f(T_{ABS}, P_{EVA}, Qu_{ABS}) \quad (18)$$

$$x_{ABS} = f(T_{ABS}, P_{EVA}, Qu_{ABS}) \quad (19)$$

By applying the mass and concentration conservation, mass flow rate of the generator is calculated by:

$$\dot{m}_6 = \dot{m}_8 + \dot{m}_7 \quad (20)$$

$$\dot{m}_6 x_6 = \dot{m}_8 x_8 + \dot{m}_7 x_7 \quad (21)$$

By combining the two equations, the following equation can be obtained:

$$\frac{\dot{m}_6(x_8 - x_6)}{x_8 - x_7} = \dot{m}_7 \quad (22)$$

The heat loads and exergy losses of different components are calculated by:

$$\dot{Q}_{GEN} = (\dot{m}_8 h_8 + \dot{m}_7 h_7) - \dot{m}_6 h_6 \quad (23)$$

$$\Delta\dot{E}_{GEN} = (\dot{m}_6 h_6 - \dot{m}_8 h_8 - \dot{m}_7 h_7) - T_0(\dot{m}_6 s_6 - \dot{m}_8 s_8 - \dot{m}_7 s_7) + \dot{Q}_{GEN}(1 - \frac{T_0}{T_{GEN}}) \quad (24)$$

$$\dot{Q}_{EVA} = \dot{m}_{12}(h_1 - h_{12}) \quad (25)$$

$$\Delta \dot{E}_{EVA} = \dot{m}_{12}(h_{12} - h_1) - T_0 \dot{m}_{12}(s_{12} - s_1) + \dot{Q}_{EVA}(1 - \frac{T_0}{T_{EVA}}) \quad (26)$$

$$\dot{Q}_{CON} = \dot{m}_{10}(h_{11} - h_{10}) \quad (27)$$

$$\Delta \dot{E}_{CON} = \dot{m}_{10}(h_{10} - h_{11}) - T_0 \dot{m}_{10}(s_{10} - s_{11}) - \dot{Q}_{CON}(1 - \frac{T_0}{T_{CON}}) \quad (28)$$

$$\dot{Q}_{ABS} = \dot{m}_3 h_3 - (\dot{m}_1 h_1 + \dot{m}_2 h_2) \quad (29)$$

$$\Delta \dot{E}_{ABS} = (\dot{m}_1 h_1 + \dot{m}_2 h_2 - \dot{m}_3 h_3) - T_0(\dot{m}_1 s_1 + \dot{m}_2 s_2 - \dot{m}_3 s_3) - \dot{Q}_{ABS}(1 - \frac{T_0}{T_{ABS}}) \quad (30)$$

The pump work and exergy losses are given by:

$$\dot{W}_p = \dot{m}_3(h_4 - h_3) = \nu_3(P_4 - P_3)/\eta_p \quad (31)$$

$$\Delta \dot{E}_p = \dot{m}_3(h_3 - h_4) - T_0 \dot{m}_3(s_3 - s_4) + \left|\dot{W}_p\right| \quad (32)$$

The heat exchanger efficiency and exergy losses are given by:

$$\varepsilon = \frac{T_7 - T_5}{T_7 - T_4} \quad (33)$$

$$\Delta \dot{E}_{HE} = -T_0 \begin{bmatrix} \dot{m}_6(s_4 - s_6) + \\ \dot{m}_7(s_7 - s_5) \end{bmatrix} \quad (34)$$

For the throttling process in expansion valves:

$$h_5 = h_2 \quad (35)$$

$$h_{11} = h_{12} \quad (36)$$

The exergy loss of the expansion valve is calculated by:

$$\Delta \dot{E}_{EXV} = \dot{m}_{11} T_0 (s_{12} - s_{11}) \quad (37)$$

The total exergy losses of the cycle can be expressed as:

$$\dot{E}_{Total} = \Delta \dot{E}_{EJE} + \Delta \dot{E}_{GEN} + \Delta \dot{E}_{EVA} + \Delta \dot{E}_{CON} + \Delta \dot{E}_{ABS} + \Delta \dot{E}_p + \Delta \dot{E}_{HE} + \Delta \dot{E}_{EXV} \quad (38)$$

Parameters used to measure the performance of refrigerators such as coefficient of performance and energetic efficiency can be expressed as [27, 28].

$$COP = \frac{\dot{Q}_{EVA}}{\dot{Q}_{GEN} + \dot{W}_p} \quad (39)$$

$$\eta_{exe} = \frac{-\dot{Q}_{EVA}(1 - \frac{T_0}{T_{EVA}})}{\dot{Q}_{GEN}(1 - \frac{T_0}{T_{GEN}}) + \dot{W}_p} \quad (40)$$

## 3. Results and Discussion

The main assumptions to analyze this cycle are presented in Table 1.

**Table 1. The main assumption for analysis absorption-ejector cycle.**

| | |
|---|---|
| $T_0[^oC]$ | 25 |
| $P_{GEN}[bar]$ | 15 |
| $T_{GEN}[^oC]$ | 75-95 |
| $T_{EVA}[^oC]$ | 5-15 |
| $T_{CON}[^oC]$ | 21-31 |
| $T_{ABS}[^oC]$ | 30 |
| $\dot{m}_6[kg/s]$ | 1 |
| $\varepsilon[\%]$ | 90 |
| $\eta_p[\%]$ | 80 |

Based on the assumptions, a simulation program using the EES software [29] was developed. Computer simulation was carried out in order to determine the various stream properties and the amount of heat and work exchanged by the main equipment of the cycle. According to the results, the thermodynamic properties of each point are given in Table 2.. Moreover, the influence of evaporator, condenser and generator temperature on the mass flow rate, heat transfer rate, coefficient of performance and exergy analysis are shown in (Figs. 2-18) at $T_{EVA} = 5℃$ , $T_{ABS} = T_{CON} = 30℃$ and $T_{GEN} = 80℃$ .

**Table 2. The thermodynamic state of each point.**

| Point | T(◦C) | h (kJ/kg) | P (bar) | s (kJ/kgK) | x |
|---|---|---|---|---|---|
| **1** | 5.05 | 1296 | 5.16 | 4.555 | 1 |
| **2** | 35.35 | -81.46 | 5.16 | 0.37 | 0.5024 |
| **3** | 30.05 | -97.36 | 5.16 | 0.2943 | 0.5763 |
| **4** | 30.15 | -95.81 | 15 | 0.2954 | 0.5763 |
| **5** | 35.15 | -81.46 | 15 | 0.3661 | 0.5024 |
| **6** | 68.05 | 78.53 | 15 | 0.8368 | 0.5763 |
| **7** | 80.05 | 123.3 | 15 | 0.9859 | 0.5024 |
| **8** | 80.05 | 1414 | 15 | 4.544 | 1 |
| **9** | 5.05 | 1267 | 5.16 | 4.555 | 1 |
| **10** | 30.05 | 1410 | 11.67 | 4.644 | 1 |
| **11** | 30.05 | 141.8 | 11.67 | 0.4881 | 1 |
| **12** | 5.05 | 141.8 | 5.16 | 0.5099 | 1 |

### 3.1. Effect of condenser temperature

#### 3.1.1. Effect of condenser temperature on the entrainment ratio

The effect of condenser temperature on the entrainment ratio of the ejector is depicted in Fig. 2. As the figure shows, when the condenser temperature increases, entrainment ratio decreases. The reason for this is that as the condenser pressure increases, the back pressure on the ejector increases. Thus, the compression ratio (ratio of condenser pressure to evaporator pressure) is increased. Hence with the same primary vapor velocity, the entrainment of secondary vapor decreases.

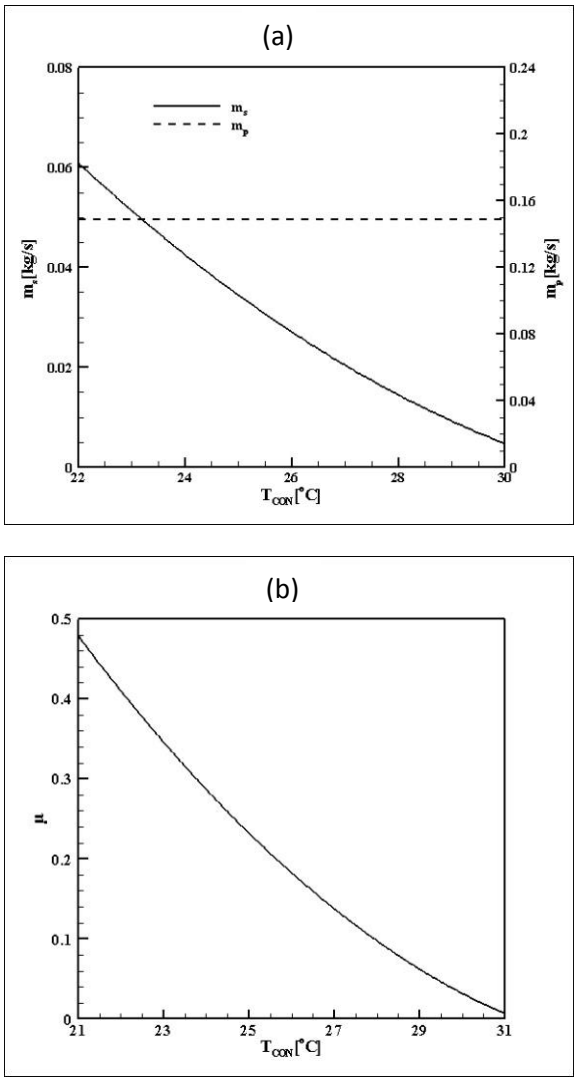


**Fig. 2. Effect of condenser temperature on the (a) primary and secondary flows (b) entrainment ratio.**

#### 3.1.2. Effect of condenser temperature on the heat rate

Fig. 3. Shows the effect of the condenser temperature on the absorber, condenser, evaporator and generator heats.

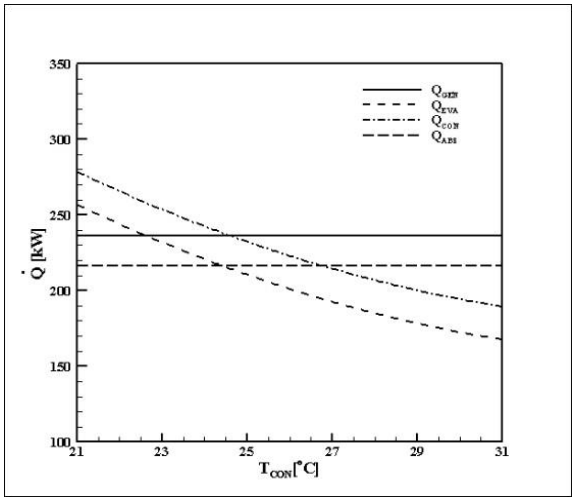


**Fig. 3. Effect of condenser temperature on the heat rate.**

It is clear that by changing the condenser temperature, enthalpy at inlet and outlet of generator, absorber, and evaporator is constant, therefore, the generator, absorber and evaporator specific heats are constant. The generator and absorber mass flow rates are constant but the evaporator mass flow decreases. Because of this, the generator and absorber's heat are constant and the evaporator's heat decreases. With increasing condenser temperature, the condenser's specific heat goes up and the condenser's mass flow rate decreases. Decreasing of mass flow rate overcomes the increasing specific heat and eventually, the condenser's heat decreases.

#### 3.1.3. Effect of condenser temperature on the COP and exergy efficiency

Fig. 4. Displays the effect of the condenser temperature on the cop and exergy efficiency. With increasing the condenser temperature, evaporator's heat decreases and generator heat is constant so COP and exergy efficiency decrease.

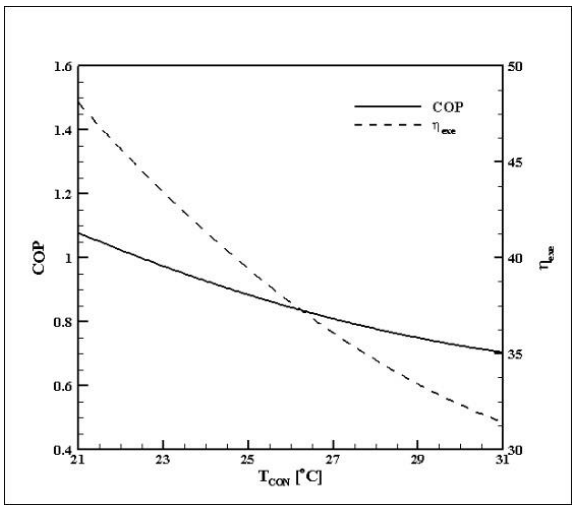


**Fig. 4. Effect of condenser temperature on the COP and exergy efficiency.**

#### 3.1.4. Effect of condenser temperature on the exergy losses

Fig. 5. Shows the effect of condenser temperature on the total exergy loss of the cycle. According to the figure, increasing the condenser temperature causes the reduction of the exergy loss.

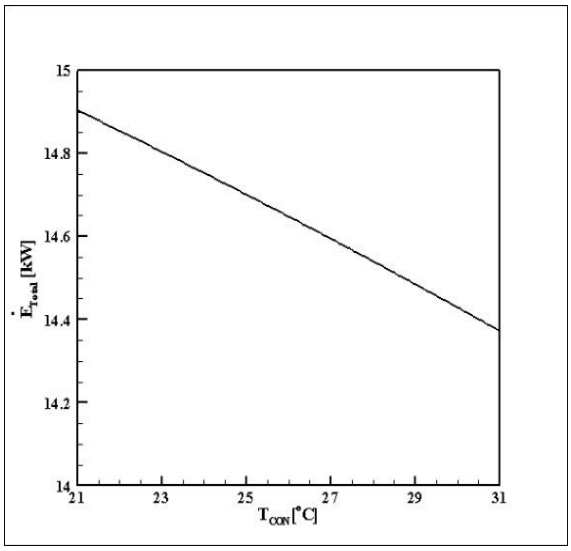


**Fig. 5. Effect of condenser temperature on the exergy losses.**

### 3.2. Effect of absorber temperature

#### 3.2.1. Effect of absorber temperature on the entrainment ratio

Fig. 6. Illustrates the effect of the absorber temperature on the entrainment ratio. With absorber temperature raises, solution concentration at absorber exit reduces and the inlet mass flow rate of absorber increases and primary mass flow rate decreases. Decreasing the primary mass flow rate induces the secondary mass flow and secondary mass flow rate decreases.

#### 3.2.2. Effect of absorber temperature on the heat rate

When the absorber temperature increases, the inlet and outlet enthalpy of condenser and evaporator are constant but the mass flow rate of condenser and evaporator decreases so heat rate of condenser and evaporator reduces. Moreover, the absorber and generator heat decrease with increasing absorber temperature which can be seen in Fig. 7.

#### 3.2.3. Effect of absorber temperature on the COP and exergy efficiency

Fig. 8. Shows the effect of absorber temperature on the COP and exergy efficiency. With increasing absorber temperature, both generator and evaporator heat rates decrease which causes the decrease in COP and exergy efficiency.

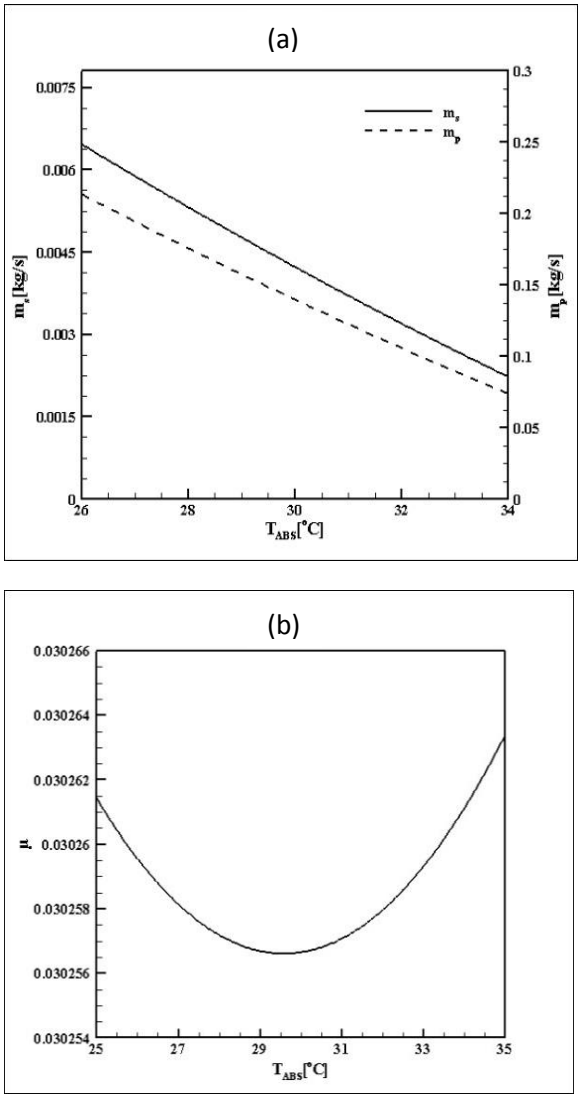


**Fig. 6. Effect of absorber temperature on the (a) primary and secondary flows (b) entrainment ratio.**

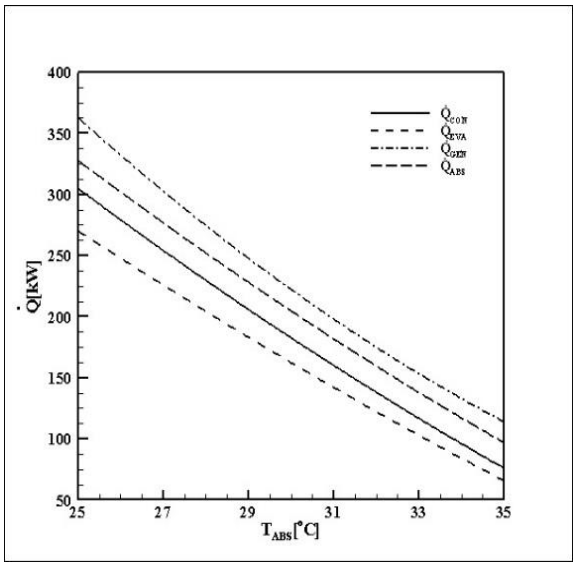


**Fig. 7. Effect of absorber temperature on the heat rate.**

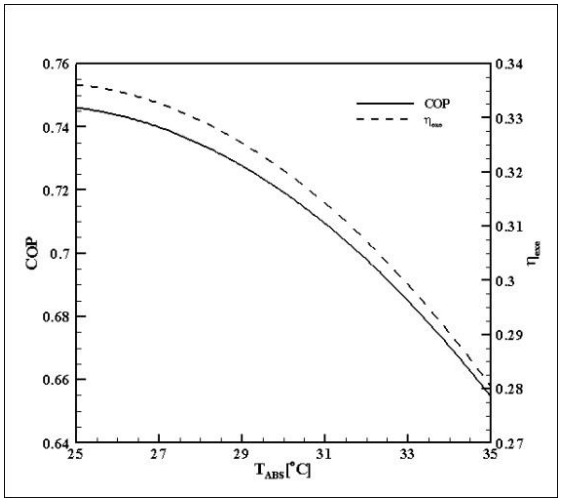


**Fig. 8. Effect of absorber temperature on the COP and exergy efficiency.**

#### 3.2.4. Effect of absorber temperature on the exergy losses

The total exergy loss decreases with increasing absorber temperature which can be seen in Fig. 9.

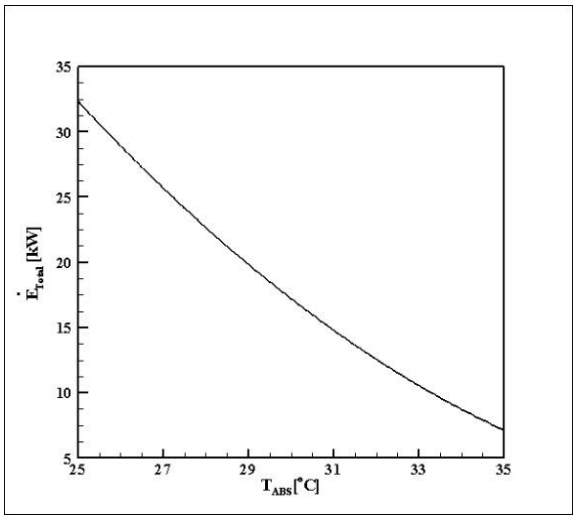


**Fig. 9. Effect of absorber temperature on the exergy losses.**

### 3.3. Effect of evaporator temperature

#### 3.3.1. Effect of evaporator temperature on the entrainment ratio

Fig. 10. Indicates the effect of the evaporator temperature on the entrainment ratio. With increasing the evaporator temperature entrainment ratio increases. This increase of the entrainment ratio is due to an increase of the secondary flow velocity by the increasing evaporator pressure.

#### 3.3.2. Effect of evaporator temperature on the heat rate

Fig. 11. Shows the Effect of evaporator temperature on the heat rate. With the increase in evaporator temperature, it is clear that the evaporator heat increases. Also, absorber, generator, and condenser heat rates increase which causes the increase in condenser mass flow rate.

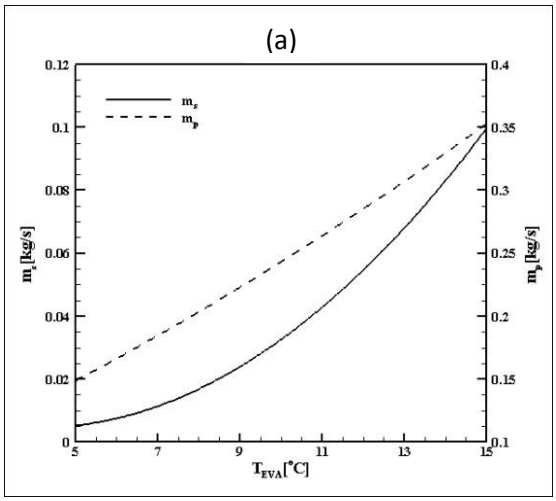


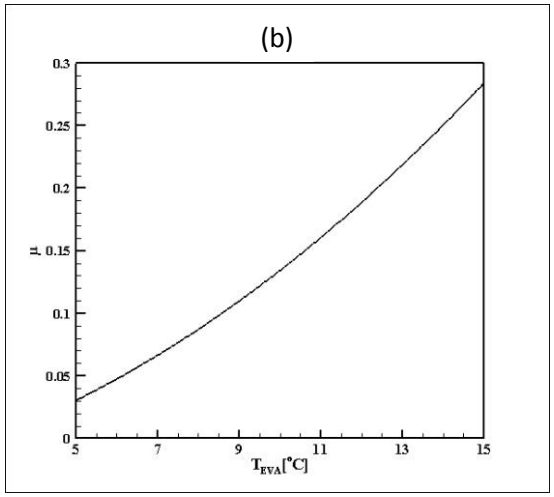


**Fig. 10. Effect of evaporator temperature on the (a) primary and secondary flows (b) entrainment ratio.**

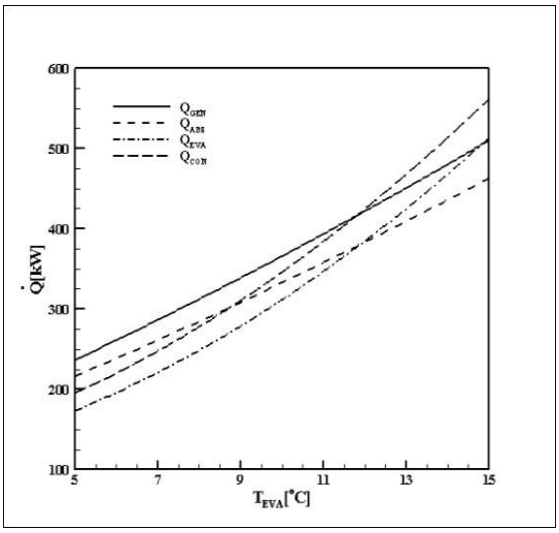


**Fig. 11. Effect of evaporator temperature on the heat rate.**

#### 3.3.3. Effect of evaporator temperature on the COP and exergy efficiency

Fig. 12. Shows the effect of evaporator temperature on the COP and exergy efficiency. It is shown that COP increases with increasing evaporator temperature but maximum energetic efficiency is achieved at lower values of the evaporator temperature so by increasing the evaporator temperature, exergy efficiency decreases.

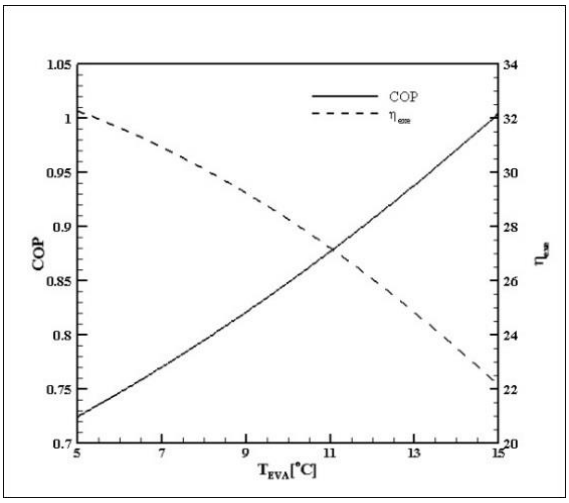


**Fig. 12. Effect of evaporator temperature on the COP and exergy efficiency.**

#### 3.3.4. Effect of evaporator temperature on the exergy loss

Fig. 13. Illustrates the effect of evaporator temperature on the total exergy losses. With increasing the evaporator temperature, the total exergy losses rate increases.

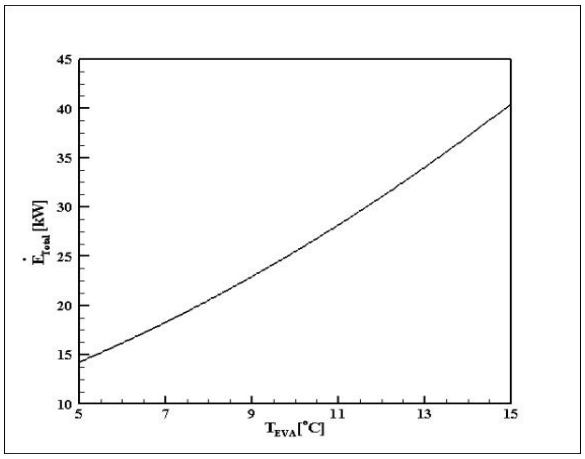


**Fig. 13. Effect of evaporator temperature on the exergy losses.**

### 3.4. Effect of generator temperature

#### 3.4.1. Effect of generator temperature on the entrainment ratio

Fig. 14. Displays the effect of the generator temperature on the entrainment ratio. With increasing the generator temperature entrainment ratio increases. This increase of the entrainment ratio is due to an increase of the primary flow velocity by the increasing generator pressure.

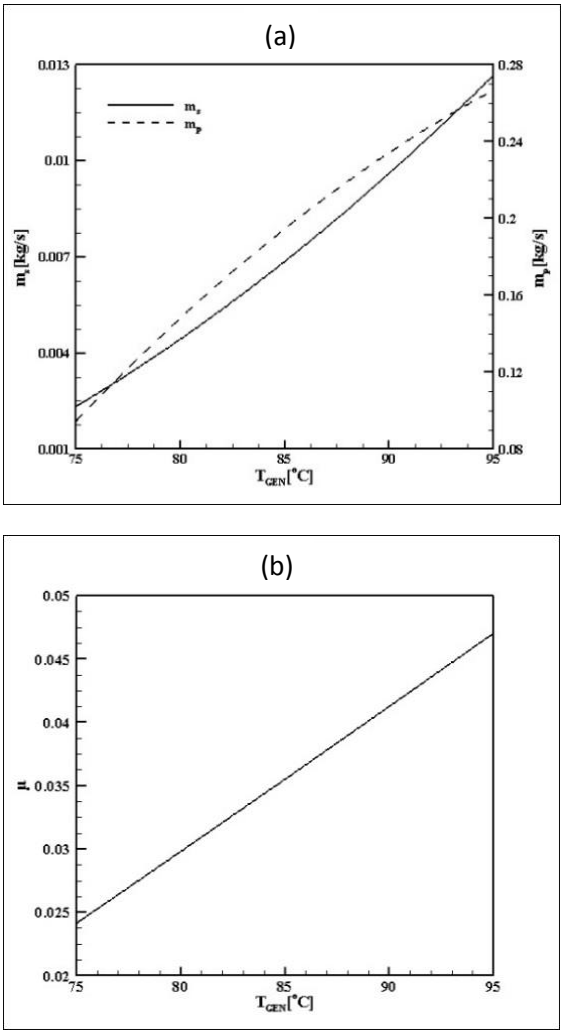


**Fig. 14. Effect of generator temperature on the (a) primary and secondary flows (b) entrainment ratio.**

#### 3.4.2. Effect of generator temperature on the heat rate

Fig. 15. Indicates the effect of generator temperature on the heat rate. The generator and absorber heat increase by increasing generator temperature. The condenser and evaporator heat rates increase, because of this the mass flow rate rises. The enthalpy at inlet and outlet of condenser and evaporator are constant.

#### 3.4.3. Effect of generator temperature on the COP and exergy efficiency

Fig. 16. Indicates the effect of generator temperature on the COP and exergy efficiency. The term $(1-\frac{T_0}{T_g})$ increases with increasing generator temperature and also generator heat rate increases, so the exergy efficiency decreases.

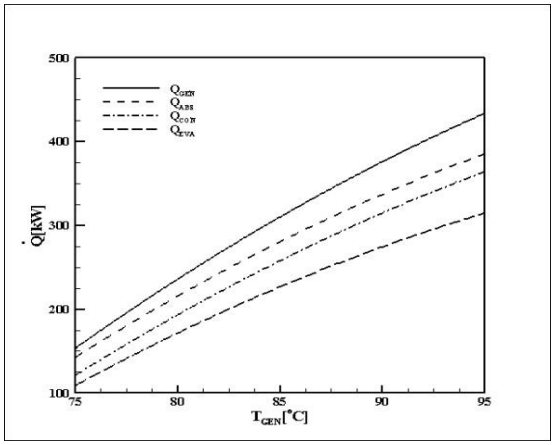


**Fig. 15. Effect of generator temperature on the heat rate.**

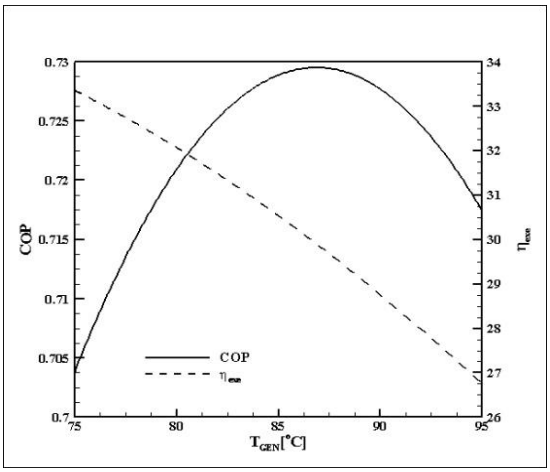


**Fig. 16. Effect of generator temperature on the COP and exergy efficiency.**

#### 3.4.4. Effect of generator temperature on the exergy loss

Fig. 17. Displays the effect of the generator temperature on the total exergy loss. It is shown that the exergy loss increases with increasing the generator temperature.

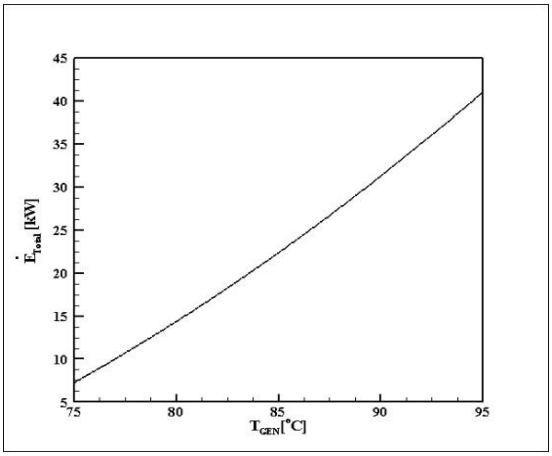


**Fig. 17. Effect of generator temperature on the exergy losses.**

#### 3.5. Exergy losses for all components

Fig. 18. Shows the exergy destruction percent for various components. The highest exergy losses at the $T_e = 5℃$ , $T_a = T_c = 30℃$ and $T_g = 80℃$ occur in the absorber, ejector, and generator, respectively. Because of the temperature difference between the absorber and the surroundings, the absorber has the highest exergy loss. Mixing of two fluids at two different temperatures and high velocity in the ejector are reasons that the ejector has the next largest loss.

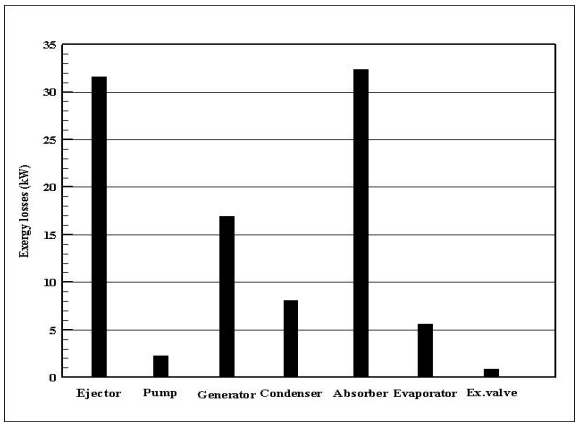


**Fig. 18. Exergy losses for different components.**

## 4. Conclusions

In this study, the first and the second law of thermodynamics is applied to ejector absorption cycle. A basic thermodynamic analysis of the $NH_3$–$H_2O$ absorption-refrigeration cycle has been performed and the dimensionless total exergy loss and exergy loss of each component and exergy efficiency and COP are calculated. The main results from this study at the defined ranges are as follows:

1. By increasing condenser temperature, the entrainment ratio, COP, exergy efficiency and exergy loss of the system decrease.
2. When the absorber temperature rises, the entire studied parameters decreases except entrainment ratio that first decreases and then increases.
3. Increasing evaporator temperature causes an increase in entrainment ratio, COP and total exergy loss and a decrease in exergy efficiency.
4. As the generator temperature goes up, the entrainment ratio and total exergy loss increase but the exergy efficiency of the cycle decrease. According to the results, COP first increases then decreases as the generator temperature rises.

## References

[1] J. Fernandez-Seara, M. Vazquez, Appl. Therm. Eng., 21(2001), 343.
[2] X. J. Zhang, R. Z. Wang, Appl. Therm. Eng., 22(2002), 1245.

[3] L. Kairouani, E. Nehdi, Appl. Therm. Eng., 26(2006), 288.
[4] M. Jelinek, A. Levy and I. Borde, Appl. Therm. Eng., 42(2012), 2.
[5] S. F. Lee, S. A. Sherif, Int. J. Energ. Res., 25(2001), 1019.
[6] M. M. Talbi, B. Agnew, Appl. Therm. Eng., 20(2000), 619.
[7] D. Hong, L. Tang, Y. He and G. Chen, Appl. Therm. Eng., 30(2010), 2045.
[8] C. Vereda, R. Ventas, A. Lecuona and M. Venegas, Appl. Energ., 97(2012), 305.
[9] G. K. Alexis, E. D. Rogdakis, Appl. Therm. Eng., 22(2002), 97.
[10] A. Sözen, T. Menlik and E. Özbas, Appl. Therm. Eng., 33(2012), 44.
[11] L. T. Chen, Appl. Energ., 30(1988), 37.
[12] A. Levy, M. Jelinek and I. Borde, Appl. Energ., 72(2002), 467.
[13] J. Wang, G. Chen and H. Jiang, Int. J. Energ. Res., 22(1998), 733.
[14] L. Shi, J. Yin, X. Wang and M. S. Zhu, Appl. Energ., 68(2001), 161.
[15] M. M. Rashidi, O. Anwar, Bég and A. Aghagoli, Int. J. Appl. Math. Mech., 8(2012), 1.
[16] G. Besagni, R. Mereu and F. Inzoli, Renew. Sust. Energ. Rev., 53(2016), 373.
[17] J. Chen, S. Jarall, H. Havtun and B. Palm, Renew. Sust. Energ. Rev., 49(2015), 67.
[18] S. Rao, G. Jagadeesh, Appl. Therm. Eng., 78(2015), 289.
[19] F. Kong, H. Kim and T. Setoguchi, JV, 4(2015).
[20] F. Mazzelli, A. Milazzo, Int. J. Refrig., 49(2015), 79.
[21] K. Śmierciew, D. Butrymowicz, R. Kwidziński and T. Przybyliński, Appl. Therm. Eng., 78(2015), 630.
[22] M. Dennis, T. Cochrane and A. Marina, Sol. Energy, 115(2015), 405.
[23] T. Zegenhagen, F. Ziegler, Int. J. Refrig., 56(2015), 173.
[24] J. Bao, Y. Lin and G. He, Int. J. Refrig., (2017).
[25] J. Szargut, D. R. Morris and F. R. Steward: Exergy analysis of thermal, chemical, and metallurgical processes, Hemisphere Publishing Corporation, New York, (1988).
[26] A. Bejan: Advanced engineering thermodynamics, Wiley, New York, (1988).
[27] A. Sozen, Energ. Convers. Manage, 42(2001), 1699.
[28] M. Kilic, O. Kaynakli, Energy, 32(2007), 1505.
[29] S. A. Klein, Engineering equation solver version 8.414., professional version, McGraw-Hill, (2009).